Journal of Power Sources 400 (2018) 533–538

Contents lists available at ScienceDirect

Journal of Power Sources

journal homepage: www.elsevier.com/locate/jpowsour

Quantification of bio-anode capacitance in bioelectrochemical systems using Electrochemical Impedance Spectroscopy

Annemiek ter Heijne[a,*], Dandan Liu[a], Mira Sulonen[b], Tom Sleutels[c], Francisco Fabregat-Santiago[d,**]

[a] Sub-department of Environmental Technology, Wageningen University, Bornse Weilanden 9, P.O. Box 17, 6700 AA, Wageningen, the Netherlands
[b] Department of Chemistry and Bioengineering, Tampere University of Technology, P.O. Box 541, FI-33101, Tampere, Finland
[c] Wetsus, European Centre of Excellence for Sustainable Water Technology, Oostergoweg 9, P.O. Box 1113, 8900 CC, Leeuwarden, the Netherlands
[d] Institute of Advanced Materials, Departament de Física, Universitat Jaume I, Av. Sos Baynat S/n, 12006, Castelló de La Plana, Spain

HIGHLIGHTS

- Fluorinated Tin Oxide (FTO) anodes with electro-active biofilm produced 1.1 A m^{-2}.
- Impedance spectroscopy was used to quantify biofilm capacitance.
- Biofilm capacitance reached 450 μF cm^{-2} while FTO capacitance was 25 μF cm^{-2}.
- Average biofilm yield of 0.55 g COD biomass/mol e^- was determined.

ARTICLE INFO

Keywords:
Electrochemical Impedance Spectroscopy
Bioanode
Microbial fuel cell
Capacitance
Biomass yield
BES
MET

ABSTRACT

Understanding the electrochemical properties of bio-anodes is essential to improve performance of bioelectrochemical systems. Electrochemical Impedance Spectroscopy (EIS) is often used to study these properties in detail. Analysis of the EIS response, however, is challenging due to the interfering effect of the large capacitance of typically used graphite and carbon-based electrodes. In this study, we used flat electrodes made of conductive Fluorine-doped Tin Oxide (FTO) as anode, and monitored bio-anode performance. We show that with this configuration, it is possible to accurately separate the distinct contributions to the electrical response of the bio-anodes: charge transfer, biofilm and diffusion resistances, and biofilm capacitance. We observed that the capacitance of the biofilm increased from 2 μF cm^{-2} to 450 μF cm^{-2} during biofilm growth, showing a relationship with current and total produced charge. These results suggest that biofilm capacitance is a measure for the amount of active biomass in bioelectrochemical systems. At the end of the experiment, the biofilm was harvested from the FTO electrode and an average yield of 0.55 g COD biomass/mol e^- was determined.

1. Introduction

Bio-anodes play an essential role in Bioelectrochemical systems (BESs) which can be used to recover electricity or produce chemicals from wastewater [1–3]. These bio-anodes are capable of extracellular electron transfer through direct and indirect mechanisms [4–6], and also of temporary charge (energy) storage in the form of electrons in multi-heme *c*-type cytochromes [7,8] or as organic polymeric molecules inside the bacterial cell [9]. All these processes together determine the rate and efficiency at which electrical current is produced. Quantification of these processes, like biofilm capacitance, charge transfer, biofilm and diffusion resistances [10–13], is essential for further development of BESs.

Electrochemical Impedance Spectroscopy (EIS) is often proposed as a powerful tool to separate these processes occurring in the bio-anode. EIS is based on the measurement of the response of a small alternating voltage (AC) perturbation at a given electrode potential. These EIS measurements are performed at different frequencies to reveal the characteristic response times of the different processes occurring in the bio-anode. Although the EIS measurement itself is relatively simple and can be performed in-situ, interpretation of the frequency dependent response is challenging. For accurate analysis, it is essential that the

* Corresponding author.
** Corresponding author.
E-mail addresses: annemiek.terheijne@wur.nl (A.t. Heijne), fabresan@uji.es (F. Fabregat-Santiago).

https://doi.org/10.1016/j.jpowsour.2018.08.003
Received 1 November 2017; Received in revised form 16 July 2018; Accepted 1 August 2018
Available online 25 August 2018

equivalent circuit that is used to interpret the data is an accurate physical representation of the system under study. Verification of the suitability of the equivalent circuit, e.g. by changing experimental settings and analyzing the response, is therefore crucial [10,12,14].

A special challenge in EIS analysis arises when the electrode under study has a high capacitance. This electrode capacitance can be of such magnitude that it is impossible to distinguish between biofilm capacitance and electrode capacitance. Even more, it may result in an overlapping response of charge transfer and diffusion processes, so that their separate contribution to the total impedance cannot be quantified [14]. So far, EIS studies on bio-anodes have been performed on porous electrodes that have high capacitance such as carbon-based plates, graphite felt, and carbon cloths [11,13,15]. Often, it remains unclear if the reported values for biofilm capacitance are related to electro-active biofilm, electrode, or the combination of both. In addition, the other resistances in the system may not be analyzed correctly when electrode capacitance is high, as high electrode capacitance will interfere with ionic diffusion in the EIS spectrum.

The aim of this study was, therefore, to quantify bio-anode properties, more specifically biofilm capacitance, charge transfer, biofilm and diffusion resistances, without interference of electrode capacitance. For this purpose, Fluorinated Tin Oxide (FTO) was used as electrode material to grow the electro-active biofilm on. Flat FTO is an attractive electrode material for electrochemical analysis of bio-anodes, because it is very stable and has a much lower capacitance, in the order of tens of $\mu F\ cm^{-2}$ [16], than typical carbon electrodes like graphite plates ($\sim 1\ mF\ cm^{-2}$) [11,17–19]. In this work, the development of an electro-active biofilm on FTO was monitored using EIS and polarization experiments. An equivalent circuit model is proposed to analyze the experimental data and to quantify electrochemical properties of the bio-anodes. Two independent experiments were performed to confirm the validity of the results.

2. Materials & methods

2.1. Bioelectrochemical system set-up with the FTO anode

Two independent experiments were performed, in which electro-active biofilms were grown on FTO electrodes. Bio-anode performance was studied for 25 days in the first experiment, and for 52 days in the second experiment. A two-chamber BES was used, each chamber having a volume of 35 mL and a projected (circular) surface area of $19\ cm^2$. The anode and cathode chamber were separated by a cation exchange membrane (FumaTech GmbH, Germany). 3.2 mm thick glass plates coated with fluorinated tin oxide (FTO) (provided by Xop Fisica, Spain) with 15 Ω/sq sheet resistance was used as anode electrode. Graphite felt of 2.8 mm thickness (CGT Carbon GmbH, Germany) was used as cathode electrode. The current collector was a 0.3 mm platinum wire for the anode, and a 0.8 mm titanium wire for the cathode. An Ag/AgCl/3 M KCl (+0.205 V vs. SHE) reference electrode was placed in the anode chamber, in between the electrode and the membrane. All potentials are reported vs Ag/AgCl.

2.2. Inoculation and media composition

Both experiments were started with clean electrodes and membranes and the BESs were inoculated with a mixed culture of anodic microorganisms from a BES fed with acetate. The anolyte contained $820\ mg\ l^{-1}\ CH_3COONa$ (10 mM acetate), $0.2\ g\ l^{-1}\ NH_4Cl$, $0.13\ g\ l^{-1}$ KCl, $1\ ml\ l^{-1}$ vitamin and $1\ ml\ l^{-1}$ mineral solution [20] in a phosphate buffer solution ($4.58\ g\ l^{-1}\ Na_2HPO_4$ and $2.77\ g\ l^{-1}\ NaH_2PO_4{\cdot}2H_2O$ (50 mM)). The anolyte was sparged with N_2 for 30 min before introducing it into the BES. The catholyte contained 100 mM potassium hexacyanoferrate[III] in a 50 mM phosphate buffer solution. Both anolyte and catholyte were recirculated via a bottle (500 mL) from the bottom to the top of the chamber with pump speeds of 70 mL min^{-1} and 100 mL min^{-1} 500 mL of the 530 mL total anolyte volume was regularly replaced with fresh medium to ensure sufficient nutrients and acetate, and stable pH (6.9–7.1). The reactor was operated inside a temperature controlled cabinet at 30 °C.

2.3. Electrochemical control and measurements

In both experiments, the anode potential was controlled at −0.35 V vs Ag/AgCl by a potentiostat (Ivium n-stat with IviumSoft v.2.462, Eindhoven, The Netherlands) in a three electrode setup, with the anode as working electrode, Ag/AgCl as the reference electrode, and the cathode as counter electrode. The anode potential of −0.35 V was chosen, as at this potential it is possible to observe the different contributions to charge transfer without excessive interference from diffusion in the EIS spectra. Bio-anode performance was characterized using EIS measurements (typically repeated 3 times; in some cases 2 or 4 times) and polarization curves, both of which were recorded at least once every 3 days. EIS measurements were performed at the same controlled anode potential of −0.35 V. An amplitude of 10 mV was used for the AC signal in a frequency range of 10 kHz–50 mHz. For some experiments, lower frequencies down to 5 mHz were used to visualize the full spectrum, including diffusion. After each EIS measurement, a polarization curve was measured. During the polarization curve, the anode potential was increased from −0.45 V to −0.30 V with each step of 0.05 V lasting for 5 min. The current was recorded each second, and the average current of the last 10 s at each anode potential was used for presentation in the polarization curves.

2.4. Electro-active biofilm quantification

At the end of the second experiment, the electro-active biofilm was removed from (scraped off) the FTO electrode to determine the total biomass weight (in g of COD). The biomass was homogenised in 10 mL of mili-Q water by ultrasound treatment prior to analysis of the chemical oxygen demand (COD) with a cuvette test (Hach Lange).

3. Results and discussion

3.1. Bio-anode performance on FTO

Two independent experiments were performed in order to confirm the validity of our analyses. In both cases an electro-active biofilm was grown on the FTO electrode, at constant anode potential of −0.35 V vs Ag/AgCl. First of all, the general performance in terms of current density and polarization behaviour is analyzed, to get a general insight in performance of the electro-active biofilm on FTO electrodes.

Fig. 1A shows the current density as a function of time for both experiments. In the first experiment, the onset of current production was on day 5, followed by a steep rise in current on day 13. In the second experiment, the onset of current production was on day 13, followed by a steep rise in current on day 21. This delay in the onset was attributed to the early replacement of medium and subsequent dilution of inoculum. The maximum current density was $0.74\ A\ m^{-2}$ for experiment 1, and $1.1\ A\ m^{-2}$ for experiment 2.

A selection of the polarization curves, obtained for experiment 2, is presented in Fig. 1B. The polarization curves showed a similar increase in bio-anode performance with time. In experiment 1, the maximum current density reached in the polarization experiment was $1.1\ A\ m^{-2}$ (day 26) at −0.30 V. In experiment 2, the maximum current density was $1.6\ A\ m^{-2}$ (day 51) at −0.30 V. The current achieved on this flat surface with low capacitance is comparable to the current achieved on other, more capacitive electrode materials, like 2D graphite-based electrodes [21]. FTO is thus a suitable electrode material to grow highly active electro-active biofilms, despite its low specific surface area and smooth surface.

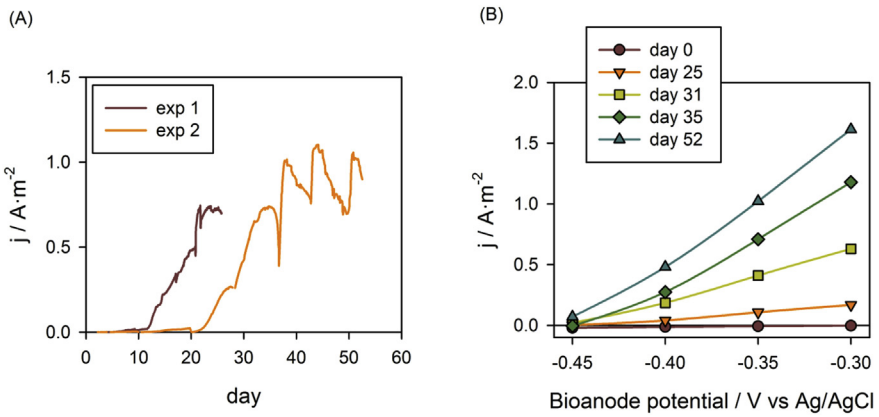

Fig. 1. (A) Evolution of current density with time for the two experiments. The steep drops in current are the result of medium replacements that were done to prevent limitations in nutrients, acetate and buffer capacity. Later start-up of the bio-anode in experiment 2 could be caused by earlier medium replacement and possible washout of active microorganisms. (B) Polarization curves (selected time points of experiment 2) show increase in biofilm activity with time.

3.2. Analysis of biofilm capacitance from EIS spectra

EIS measurements were done to gain insight in bio-anode properties and the development of the electro-active biofilm during growth. Thus, EIS spectra were measured and analyzed at different growth stages of the electro-active biofilms at −0.35 V. The trends observed in the Nyquist plots for both experiments are similar (detailed plots for experiment 1 are provided in Figure S2, ESI). In the first days after inoculation when no current was produced yet, a nearly straight line was observed (Fig. 2A), that evolved to a large arc in the next few days (see Figure S2, ESI) [22]. This line has its origin in a high total internal resistance, that is related to limited charge transfer reactions, as there is no active biofilm yet present on the electrode. As time advanced, and current production by the biofilm increased, the formation of a deformed arc was observed, its total width decreasing with time. With increasing time (and current generation), this deformed arc at high frequency splits in two different features, see Fig. 2B, which allows the identification of new phenomena occurring in the active biofilm. These three arcs were observed in several other measurements, once the biofilm was sufficiently matured (Figure S3, ESI).

EIS spectra were fitted with the equivalent circuit presented in Fig. 3, that combines processes occurring in the biofilm, electrode, the electrolyte and their interfaces. R_{el} and R_b represent the electric resistance of the FTO electrode and the ionic resistance of the bulk anolyte, the sum of which will be measured as a single ohmic resistance in series with the rest of the elements, see Figure S3A. This series resistance, $R_s = R_{el} + R_b$ provides the intersection with Z' axis at high frequencies, see Fig. 2B.

The high frequency arc is associated with the parallel combination of a capacitance, C_{FTO}, which accounts for charge accumulation at the interface of the FTO electrode and the solution interface, and a resistor, R_{bio}. This R_{bio} has two possible contributions: the charge transfer resistance at the interface between the FTO electrode and the electro-active biofilm and the transport resistance of electrons in this electro-active biofilm. The second arc at intermediate frequencies is associated with the combination of the biofilm capacitance (C_{bio}) and the charge transfer resistance (R_{ct}) between solution and electro-active biofilm, which is related to acetate oxidation. The low frequency arc is related to diffusion of reacting species in the vicinity of the electro-active biofilm, most importantly acetate and protons. It is described by the diffusion term of the impedance (Z_d):

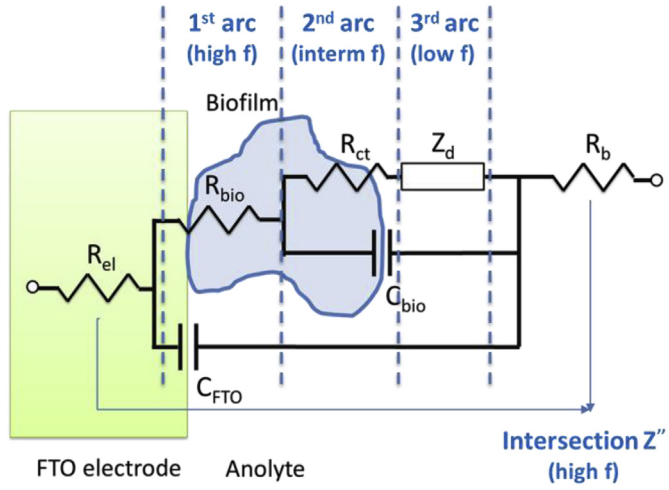

Fig. 3. The equivalent circuit that represents the bio-anode, which is used to analyze the EIS spectra and its relation to the different frequency ranges.

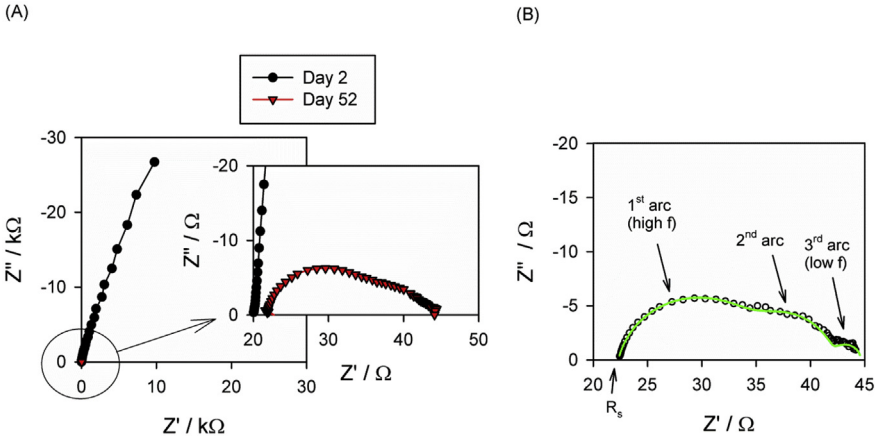

Fig. 2. (A) First days, the total internal resistance is very large and the arc does not close, resulting in a straight upward line. Inset: after growth of the biofilm, impedance is represented by the three smaller and deformed arcs accounting for the complex equivalent circuit presented in (B) Nyquist plot reveals three characteristic arcs that relate to the response at different frequencies. Data taken from day 40 of experiment 2 at −0.35 V vs Ag/AgCl.

$$Z_d = R_d \frac{\tanh(j\omega/\omega_d)^{1/2}}{(j\omega/\omega_d)^{1/2}} \quad (1)$$

where R_d is the diffusion resistance, $j = \sqrt{-1}$, ω is the (angular) frequency of the measurement and $\omega_d = D/L^2$ the diffusion frequency, with D the diffusion coefficient and L the thickness of the diffusion boundary layer. While Z_d is not always clearly visible, under certain conditions, its characteristic spectrum is clearly observed (see Figure S1, ESI).

The equivalent circuit proposed in Fig. 3 is an evolution of a previous equivalent circuit used to fit EIS data of biofilms deposited onto carbon electrodes [11,18,22]. Carbon electrodes present very high capacitances ($\sim 1\ mF\ cm^{-2}$) and this fact effectively masks other capacitive processes occurring in the biofilm. The intentional use of a low capacitance electrode as FTO reveals a higher complexity in the electrical response of biofilm than the simple charge transfer resistance (R'_{ct}) used in these previous models based on Randles equivalent circuit, see Figure S4. While Z_d presents values similar to those found in previous paper [22], the fact that the high frequency arc becomes more and more deformed until allowing distinguishing two arcs, indicates the presence of a new capacitor that increases with time and biofilm activity. At the same time this new capacitance allows decoupling R'_{ct} in several contributions. Under these premises, the most likely equivalent circuit found substitutes R'_{ct} by the combination of R_{bio}, R_{ct} and C_{bio} shown in Fig. 3. Alternative equivalent circuits such those presented in Figures S3C and S3D were also tested, but results obtained did not follow the behaviour expected during the growth of the biofilm.

Analysis of these data showed that biofilm capacitance (C_{bio}) could be separated from electrode (FTO) capacitance (C_{FTO}) in the EIS spectra. A control experiment, with an FTO electrode without electroactive biofilm showed a value of C_{FTO} of $22\ \mu F\ cm^{-2}$. Without biofilm ($C_{FTO} \gg C_{bio}$), the equivalent circuit in Fig. 1B reduces to a Randles circuit as used previously [11,18]; as C_{bio} becomes negligible and disappears from the equivalent circuit. After inoculation, and onset of current generation, the value for C_{bio} starts increasing. For current $> 0.1\ A\ m^{-2}$, the EIS spectrum in the Nyquist plot presented up to three characteristic arcs as shown in Fig. 2B and therefore a separate value for C_{bio} could be distinguished. This distinction became more clear after biofilm growth continued and C_{bio} became larger than $10\ \mu F\ cm^{-2}$, ($2\ \mu F\ cm^{-2}$ in some cases) clear distinction was observed. In addition, at this point it becomes possible to decouple and quantify the different contibutions of R_{bio} and R_{ct}.

The results for FTO capacitance and biofilm capacitance are shown in Fig. 4. The FTO capacitance was quite constant at a value of 0.5 mF, corresponding to $25\ \mu F\ cm^{-2}$. This value was similar to the capacitance of the control experiment without biofilm ($22\ \mu F\ cm^{-2}$). It also agrees well with the Helmholtz capacitance at the interface between FTO electrode and solution [23]. The fact that C_{FTO} remains constant and at a value similar to the one of bare FTO electrode confirms the validity of equivalent circuit used. The biofilm capacitance showed a clear 2 orders of magnitude increase with time, starting from $2\ \mu F\ cm^{-2}$ and reaching $250\ \mu F\ cm^{-2}$ in experiment 1 and $450\ \mu F\ cm^{-2}$ in experiment 2. Note that shifting the analysis of the first experiment by 8.5 days, to align the start of current production in both experiments (Figure S5, ESI), we see that biofilm capacitance development is very similar for both experiments.

More porous, graphite-based electrodes have a typical capacitance of 1–3 $mF\ cm^{-2}$ [11,17–19], while the highest value found here for biofilm capacitance is roughly one order of magnitude lower. The separation between biofilm capacitance and electrode capacitance is more difficult when using electrodes with higher capacitance, in which case the biofilm capacitance may not be visible in the EIS spectra. In one other study using low capacitance gold electrodes, in which a biofilm was formed over a non-conductive gap [7], biofilm capacitance was determined using EIS. Biofilm capacitance was $620\ \mu F\ cm^{-2}$, a value in the same order of magnitude as found here. Other studies have analyzed bio-anode properties, among which anode capacitance, with and without biofilm. For example, Borole et al. [24] used EIS to characterize resistances of a graphite felt anode and reported an increase in electrode capacitance when the biofilm was present. No separation between electrode capacitance and biofilm capacitance was reported; and the equivalent circuit used did not allow such a separation between electrode and biofilm capacitance.

3.3. Relationship between current, total charge and biofilm capacitance

During both experiments, an increase in biofilm capacitance with time was found, in combination with an increase in current density (and total charge) with time. Biofilm capacitance is shown as a function of the current that was recorded during EIS in Fig. 4B and Figure S6, ESI, and as a function of total charge in Fig. 4C and D. In both experiments, biofilm capacitance increased linearly with current density, providing very similar values in the full range of measurements. This reveals the close relationship between current and biofilm capacitance. The same holds for total charge and biofilm capacitance, although the biofilm capacitance levels off at higher total charge. Current production, total charge, and biofilm capacitance are related to electroactive compounds inside the biofilm. The increase in biofilm capacitance seems related to an increase in total biofilm, or in the electroactive compounds inside the biofilm, and therefore seems related to biofilm growth. In BESs, biofilm growth is linked to the total produced charge. In the lag and exponential growth phase of BESs start-up, the increase in total charge thus coincides with the increase in biofilm and its electroactive components. These results are in line with the study on analysis of biofilm quantity on FTO electrodes in-situ using optical coherence tomography (OCT) [25]. We observed that the amount of biofilm keeps increasing linearly at constant yield, even far beyond the exponential growth phase, when the current has stabilized. This indicates that only part of the biomass is involved in current production or that a larger amount of biomass produces current less efficiently. Possibly, a combination of OCT measurements with EIS analysis to gain more insights in the ratio between active and inactive biomass, and the presence of electro-active components.

Data from capacitance are in accordance with the observation that electrons are accumulated in the bacterial membrane surface, i.e. stored in redox active components, like multi-heme *c*-type cytochromes as reported for *Geobacter sulfurreducens* [7,8], rather than in organic polymeric molecules inside the bacterial cell, where electrical perturbations to measure capacitance would have more difficulties to access. It is therefore likely that the accumulated charge in the cytochromes is compensated by ions in the solution, forming an electrical double layer that results in the measured capacitance. The measured capacitance seems to be a measure for the amount of electroactive biomass present on the electrode surface. These results open the possibility of detailed electrical study on electron storage in bacterial membranes.

3.4. Analysis of other biofilm properties from EIS spectra

In addition to biofilm capacitance, information on charge transfer resistance, biofilm resistance, and diffusion resistance can be obtained from the EIS spectra. These results are shown in Figure S7A-D, see ESI. As time proceeded, all resistances decreased, and an inverse linear relationship between current density and R_{ct} and R_{bio} was found. The linear relationship between the inverse of R_{ct} and current density was already described in previous work [22], however, this behaviour is much more evident here.

Fig. 5 shows the relationship between C_{bio} and the inverse of charge transfer resistance R_{ct} and biofilm resistance R_{bio}. There is a clear link between C_{bio} and $1/R_{ct}$, showing that charge transfer resistance (related to conversion of substrate) decreases with increasing C_{bio}. This is in accordance with the finding that C_{bio} increases with increasing current density; whereas current density is a direct measure of biofilm activity,

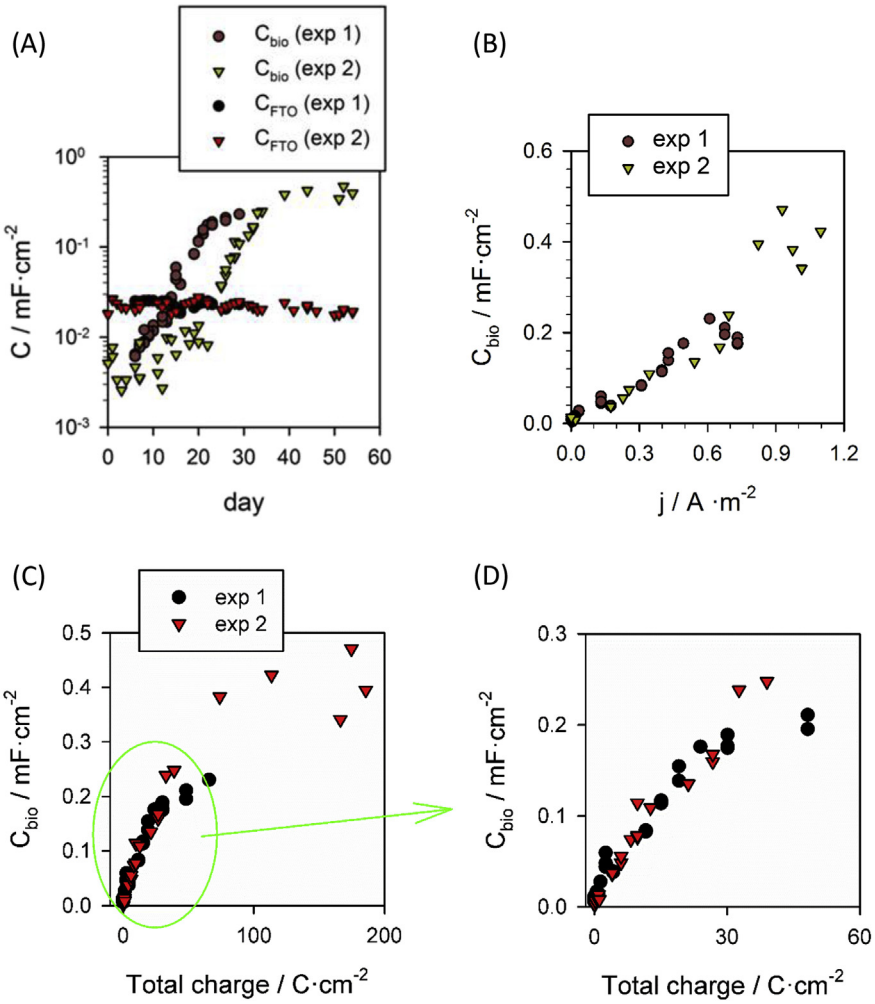

Fig. 4. (A) FTO capacitance is constant, while biological capacitance increases as a function of time. (B) Biofilm capacitance increased linearly with current density. (C) Biofilm capacitance also shows a relationship with total charge, which seems linear (D) especially in the first stage of biofilm growth.

C_{bio} is an indirect measure of biofilm activity. At the same time, C_{bio} also shows a clear link to $1/R_{bio}$ and shows that with increasing biofilm activity (that is linked to C_{bio}), the biofilm resistance decreases. The decrease in R_{bio} may be related to the increase in the surface connections between the biofilm and the FTO electrode, which would contribute in three ways: (i) an increase in the contact surface between biofilm and the FTO electrode; (ii) the increase in the number of electron conductive connections within the biofilm, that connect the increasing numbers of electro-active bacteria to each other and to the FTO electrode. This last effect could be partially compensated by an increase in transport resistance as the increasing biofilm thickness increases the distance between the bacteria in contact with the electrolyte

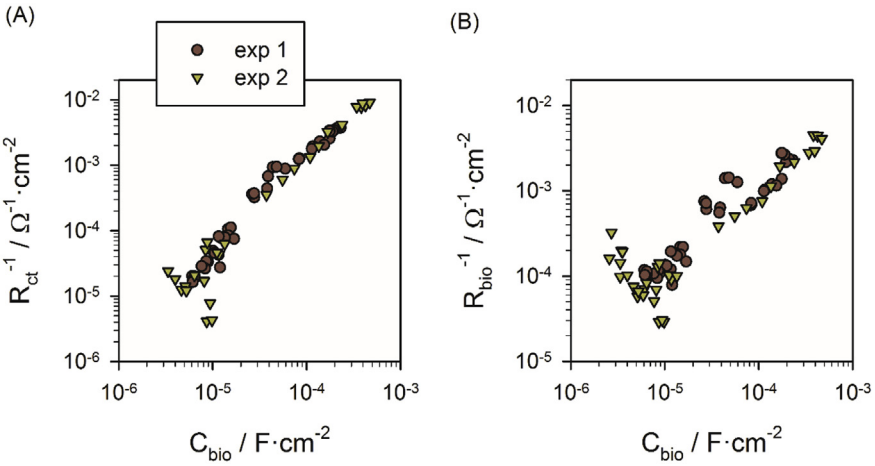

Fig. 5. Analysis of EIS spectra resulted in quantification of R_{ct} and R_{bio} (A) With increase in C_{bio}, charge transfer resistance decreases. (B) Biofilm resistance decreases with increasing C_{bio}.

and those in contact with the anode. (iii) The increase in the concentration of redox active components (e.g. c-type cytochromes) in the bacteria, easing charge transfer from bacteria to FTO. This last possibility, together with the increase in carrier concentration of redox active components (both related to C_{bio}) would result in the increase of the overall conductivity of the biofilm and thus the decrease in R_{bio}. Finally, while out of the scope of this paper, it is worth to comment on the decrease of diffusion resistance shown in Figure S5A as time and biofilm growth progresses. Possible origins of this behaviour could be a decrease in diffusion length, linked to local increase in conductivity, or an increase of diffusing species in solution close to the bacteria, both associated to the increasing biofilm activity.

3.5. Biofilm quantification

At the end of the second experiment, the cell was disassembled, and a well-developed biofilm was observed (Figure S8, ESI). The biofilm was removed from the electrode to determine biofilm weight, and a total COD of 19 mg was measured. In combination with the total coulombs of charge transferred during the entire experimental time (34.3 mmol e^-), an average yield of 0.55 g COD biomass/mol e^- was found. This can be translated into a yield per substrate (8 mol e^-/mol acetate) of 0.069 g COD biomass/g COD acetate. The theoretical maximum biomass yield is 0.10 g COD biomass/g COD acetate, calculated at the used anode potential of −0.35 V vs Ag/AgCl (−0.15 V vs SHE) using the thermodynamic approach from Picioranu et al. [26] The average yield determined after harvesting from the FTO anode is thus slightly lower than the theoretical yield. Likely, our measurement underestimates the actual yield, as only the biomass that remained attached to the electrode throughout the 52 days experimental period was harvested and analyzed. More accurate biomass determination is underway to get more insights in biomass yields of electro-active biofilms.

3.6. Outlook for future use of FTO electrodes

FTO electrodes are not only a suitable material to quantify capacitance in combination with EIS, they also provide a means to easily remove biofilms from the electrode for further chemical or microbial analysis. In addition, their transparent nature offers new possibilities for in-situ spectroscopic analyses like Confocal Resonance Raman Microscopy, as has been shown for electro-active biofilms on similar Indium Tin Oxide (ITO) electrodes [8,27]. EIS on FTO electrodes might be a suitable tool for non-invasive measurements of biofilm density, via the analysis of capacitance. To use EIS for biofilm density measurement, a more detailed calibration between biofilm amount and biofilm capacitance is required. Combining in-situ measurements of capacitance using EIS and spectroscopic analyses, in combination with biofilm characterization, provides exciting new opportunities to gain further insights in electron transfer mechanisms and other factors that determine performance of electro-active biofilms.

4. Conclusions

In summary, we have proposed a new configuration using FTO electrodes to quantify electrochemical properties of bio-anodes with high accuracy. Using this FTO electrode, the interference from the electrode capacitance was minimized. As a result, biofilm capacitance, charge transfer, biofilm and diffusion resistances could be analyzed separately. During biofilm growth, biofilm capacitance increased from 2 μF cm^{-2} to 450 μF cm^{-2}, while FTO capacitance was 25 μF cm^{-2}. Biofilm capacitance showed a relationship with total produced charge, which was linear in the early stage of biofilm growth. In addition, FTO provides a means to analyze biofilm yields on electrodes. This procedure opens the possibility of more detailed studies about electrical interactions in biofilms in general, and charge storage in biofilms in particular.

Acknowledgements

The authors wish to acknowledge funding from the European Union Seventh Framework Programme (FP7/2012–2016) project ‘Bioelectrochemical systems for metal production, recycling, and remediation’ under grant agreement n° 282970.

AtH is supported by a NWO VENI grant n° 13631.

Appendix A. Supplementary data

Supplementary data related to this article can be found at https://doi.org/10.1016/j.jpowsour.2018.08.003.

References

[1] B.E. Logan, B. Hamelers, R. Rozendal, U. Schröder, J. Keller, S. Freguia, P. Aelterman, W. Verstraete, K. Rabaey, Environ. Sci. Technol. 40 (2006) 5181–5192.
[2] B.E. Logan, D. Call, S. Cheng, H.V.M. Hamelers, T.H.J.A. Sleutels, A.W. Jeremiasse, R.A. Rozendal, Environ. Sci. Technol. 42 (2008) 8630–8640.
[3] H.V.M. Hamelers, A. Ter Heijne, T.H.A.J. Sleutels, A.W. Jeremiasse, D.P.B.T.B. Strik, C.J.N. Buisman, Appl. Microbiol. Biotechnol. 85 (2010) 1673–1685.
[4] D.R. Lovley, Energy Environ. Sci. 4 (2011) 4896.
[5] G. Reguera, K.D. McCarthy, T. Mehta, J.S. Nicoll, M.T. Tuominen, D.R. Lovley, Nature 435 (2005) 1098–1101.
[6] D.R. Lovley, Annu. Rev. Microbiol. 66 (2012) 391–409.
[7] N.S. Malvankar, T. Mester, M.T. Tuominen, D.R. Lovley, ChemPhysChem 13 (2012) 463–468.
[8] Y. Liu, D.R. Bond, ChemSusChem 5 (2012) 1047–1053.
[9] S. Freguia, K. Rabaey, Z.G. Yuan, J. Keller, Environ. Sci. Technol. 41 (2007) 2915–2921.
[10] R.A. Yoho, S.C. Popat, F. Fabregat-Santiago, S. Giménez, A. ter Heijne, C.I. Torres, H. Beyenal, J. Babauta, Biofilms Bioelectrochemical Syst, John Wiley & Sons, Inc, Hoboken, NJ, USA, 2015, pp. 249–280.
[11] A. ter Heijne, O. Schaetzle, S. Gimenez, L. Navarro, B. Hamelers, F. Fabregat-Santiago, Bioelectrochemistry 106 (2015) 64–72.
[12] X. Dominguez-Benetton, S. Sevda, K. Vanbroekhoven, D. Pant, Chem. Soc. Rev. 41 (2012) 7228–7246.
[13] Z. Lu, P. Girguis, P. Liang, H. Shi, G. Huang, L. Cai, L. Zhang, Bioproc. Biosyst. Eng. 38 (2015) 1325–1333.
[14] A. Ter Heijne, O. Schaetzle, S. Gimenez, F. Fabregat-Santiago, J. Bisquert, D.P.B.T.B. Strik, F. Barrière, C.J.N. Buisman, H.V.M. Hamelers, Energy Environ. Sci. 4 (2011) 5035.
[15] C. Santoro, F. Soavi, A. Serov, C. Arbizzani, P. Atanassov, Biosens. Bioelectron. 78 (2016) 229–235.
[16] F. Fabregat-Santiago, G. Garcia-Belmonte, J. Bisquert, P. Bogdanoff, A. Zaban, J. Electrochem. Soc. 150 (2003) E293.
[17] R. Rousseau, M. Rimboud, M.L. Délia, A. Bergel, R. Basséguy, Bioelectrochemistry 106 (2015) 97–104.
[18] R.P. Ramasamy, Z. Ren, M.M. Mench, J.M. Regan, Biotechnol. Bioeng. 101 (2008) 101–108.
[19] A.K. Manohar, O. Bretschger, K.H. Nealson, F. Mansfeld, Bioelectrochemistry 72 (2008) 149–154.
[20] E. A. Wolin, M. J. Wolin, R. S. Wolfe, 1963, 238, 2882–2886.
[21] A. ter Heijne, H.V.M. Hamelers, M. Saakes, C.J.N. Buisman, Electrochim. Acta 53 (2008) 5697–5703.
[22] A. ter Heijne, O. Schaetzle, S. Gimenez, L. Navarro, B. Hamelers, F. Fabregat-Santiago, Bioelectrochemistry 106 (2015) 64–72.
[23] B.E. Conway, J. Electrochem. Soc. 138 (1991) 1539.
[24] A.P. Borole, D. Aaron, C.Y. Hamilton, C. Tsouris, Environ. Sci. Technol. 44 (2010) 2740–2745.
[25] S. Molenaar, T. Sleutels, J. Pereira, M. Iorio, C. Borsje, J. Zamudio, F. Fabregat-Santiago, C. Buisman, A. Ter Heijne, ChemSusChem (2018), https://doi.org/10.1002/cssc.201800589.
[26] C. Picioreanu, I.M. Head, K.P. Katuri, M.C.M. van Loosdrecht, K. Scott, Water Res. 41 (2007) 2921–2940.
[27] B. Virdis, F. Harnisch, D.J. Batstone, K. Rabaey, B.C. Donose, Energy Environ. Sci. 5 (2012) 7017.